PREPARATION AND CHARACTERIZATION OF BEADS OF FISH SCALES HYDROXYAPATITE/COLLAGEN /SILVER NANOPARTICLES BY USING INFILTRATION METHOD

Mustafa Mudhafar[1*], Ismail Zainol [2], Hasan Ali Alsailawi [1] Che Nor Aiza Jaafar[3], Ruaa Kadhim Mohammed[1], Mohammed sachit hamzah[4] and Sahi Jawad Dhahi[1]

[1]Department of Anesthesia and Intensive Care Techniques, Faculty of Al-Tuff Collage, Karbala, 56001, Iraq
[2]Department of Chemistry, Faculty of Science and Mathematics, Universiti Pendidikan Sultan Idris, UPSI Proton City, 35900 Tanjung Malim, Perak, Malaysia.
[3]Department of Mechanical and Manufacturing Engineering, Faculty of Engineering, Universiti Putra Malaysia, UPM 43000 Serdang Selangor, Malaysia
[4]Medical Laboratory Technique, Kut University College, Al-kut, Wasit, Iraq, 52001

*almosawy2014@gmail.com

Abstract. The composites of hydroxyapatite/collagen (HA/Col) were seen to be the most encouraging bone graft because of the likenesses with the natural bones .The aim of the present study was to prepared the fish scales hydroxyapatite/collagen /silver nanoparticles (FsHA/FsCol/AgNPs) as a beads by using infiltration method. FsHA/FsCol/AgNPs composites beads were prepared by using new method (infiltration), including to infiltrated of FsHA beads in the FsCol-AgNPs solution. The composites beads of the FsHA/FsCol have been modified by incorporated with AgNPs. The chemical-physical properties for the prepared beads have been evaluated by using fourier-transform infrared spectroscopy (FTIR), scanning electron microscopy (SEM), energy dispersive x-ray analysis (EDX) and x ray diffraction analysis (XRD). The results had revealed that by using XRD and FTIR analysis, the peaks of functional groups of FsCol and AgNPs were observed in the matrix of the beads. FESEM had shown the morphology of beads with intact to the availability of AgNPs on the surface of porous structure. The beads morphology demonstrated a homogeneous surface with AgNPs scattered in the matrix.

Keywords: Fish Scales, Collagen, Hydroxyapatite, Silver nanoparticles

Article Info

Received 17th September 2021
Accepted 22nd November 2021
Published 20th December 2021

ISSN: 1823-7010, eISSN: 2600-7444

Introduction

Introduction as a dynamic tissue that has the capability of remodeling. The remodeling of the bone includes bone synthesis and resorption. The cells in the bone can be classified into two main groups- osteoclasts and osteoblasts [1,2]. These two forms play essential roles in the formation of the new and the resorption of aged bone, respectively [3,4].

The bone is exposed to many defects such as injury, infection and bone tumor [5]. Some of these defects are small (i.e. 1\3 inch), and can be self-treated as the bone is a tissue that has the ability to repair itself, but there are some defects that are large (more than 1\3 inch) such as bone fractures, as well as defects that are caused by diseases and shocks, in such cases the bone cannot repair itself, which makes the substitutes of the bone to be one of the most implanted tissues in human medicine store [6,7].

The available HA is known to be chemically synthesized via chemical reaction such as chemical precipitation [8]. Nevertheless, due to the high cost related to chemicals that had been utilized in the synthetic process, other natural sources are examined to lead to economical HA production. Among the important biological sources for natural HA are fish bones, fish scales, and bones of bovine, eggshells, and snail shells [9]. However, due to animal diseases, animal diseases such as hyaline membrane disease (HMD) and mad cow disease poses a threat to the production of HA from animal bones, rendering animal-based HA not a good alternative of HA. The significant raw sources would be the fish waste, particularly fish scales [10], additionally, fishes are abundant in the environment, and the application of their byproducts is suitable for biomedical application since it would reduce environmental pollution and threats of biohazards to humans [11].

Collagen-based (Col) scaffolds are classified into three major components, Col with bio-ceramic, carbon components, and polymer components [12]. Collagen-based ceramic has been fabricated in three significant forms, such as dry powder [13], three-dimensional scaffolds [14], and hydrogels [15]. These three forms have been fabricated and cross-linked in many techniques such as freeze-drying [16]simulated body fluid (SBF) [17] also in situ synthesis as a fabricate techniques, and DHT (dehydrothermal) [18] glutaraldehyde and, genipin [19], as a cross-linking method.

HA/Col composites were investigated as a functional biomaterial, which was used in many medical applications, however, there was no report on HA/Col from the scales of fish. To fill this gap HA/Col both from scales of fish have been prepared. Based on previous studies, no research was reported on the incorporation of AgNPs in HA/collagen composites. Thus, a novel fish scales HA/Col/AgNPs composite was developed for cheaper and safer bone filler materials in this study.

Materials and Methods

Silver nitrate ($AgNO_3$) purchased from the Bendon brand (Malaysia), Leaves of *Melia dubia (neem)* were collected from Perak Malaysia, locally, Collagen, and hydroxyapatite from the scales of the fish, produced by our chemistry lab, chemistry department UPSI, Perak, Malaysia. The Genipin cross liker has been purchased from Xian Lyplar biotech co. China

The preparation process of FsHA and Porous FsHA beads. The 3 mm beads of FsHA and FsHA/Starch (St) were prepared using the agglomeration technique. FsHA powder was crushed to obtain powder without any cloves, then distilled water was sprayed over the powder, and the size was formed approximately 3 mm. Beads of FsHA were placed in the mold and oven-dried at 80 °C. A similar procedure was used to prepared beads of 80:20 wt% and 20:80 wt% FsHA: St. The beads of FsHA and FsHA/St were sintered at 1200 °C for 2 h in the furnace.

The preparation process of Beads with FsCol-AgNPs. FsHA/FsCol/AgNPs beads were prepared by using infiltration method. Briefly, 0.1 g of FsCol were dissolved in 100 mL distilled water and mixed properly until a clear solution was obtained. Beads of FsHA were submerged in the solution of FsCol at room temperature overnight to allow penetration of the liquid molecules inside the voids. To prepare FsHA/FsCol/AgNPs beads whereby 0.1 g FsCol and 0.05% AgNPs have been used to obtain 0.1% (w/v) of FsCol-AgNPs solution. FsHA beads were immersed inside FsCol-AgNPs solution at room temperature overnight. Genipin was used as a cross-linker agent to cross-link collagen in the beads. Approximately 0.03 M genipin was prepared, and the sample was immersed in the genipin solution to cross-link collagen in the beads and dried in the oven at 50 °C. The obtained beads were washed two to three times with distilled water to obtain the final product.

Characterization of FsHA/FsCol, FsHA/FsCol/AgNPs beads. The beads of FsHA/FsCol and FsHA/FsCol/AgNPs have been characterized using several techniques such as Fourier-transform infrared spectroscopy (FTIR), scanning electron microscope (SEM), energy-dispersive X-ray (EDX) spectroscopy, and X-ray powder diffraction (XRD).

Results and Discussion

FTIR patterns of FsHA/FsCol/AgNPs beads. The starting materials used to prepare FsHA/FsCol/AgNPs beads have been analyzed through FTIR analysis. Figure 1 a, b, and c show the FTIR spectrum of AgNPs, FsCol and FsHA, respectively. The spectrum in Figure 1 c shows the functional group peaks of FsHA and the hydroxyl group. The OH showed a sharp peak at around 3552 cm^{-1} and a weak peak at 642 cm^{-1}. Meanwhile, a broad peak at 1043 cm^{-1} displayed a single band for the phosphate group, and the peak at 1092 $cm^{-1.}$ For the phosphate group (PO_4^{3-}). Triplet peaks at around 507 to

606 cm^{-1} corresponding to the PO_4^{3-} bending vibration were observed [20,21]. Figure 1 b shows the functional groups of FsCol. The strong band was monitored at 3446 cm^{-1} and 1646 cm^{-1}, which referred to be as amide A (N-H) and amide I (C=O), respectively.

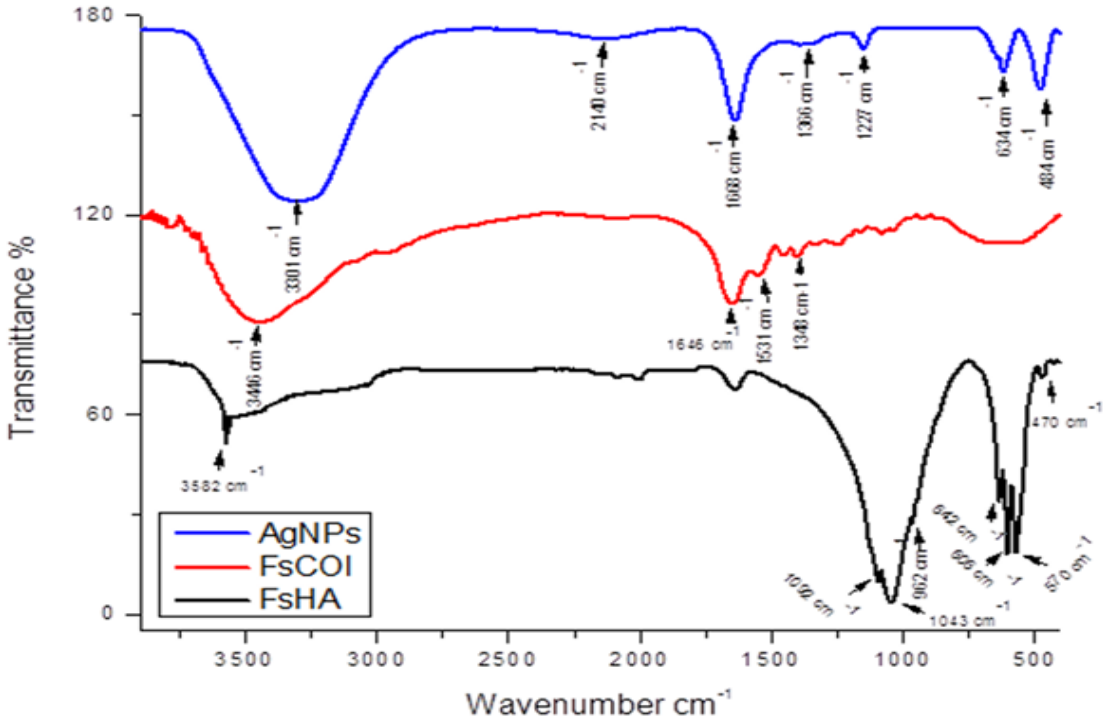

Figure 1. FTIR Spectra for (a) AgNPs, (b) FsCol and (c) FsHA

Figure 1a The absorbance peaks at 1531 cm^{-1} (N-H band from amide III) and 1348 cm^{-1} (CN band from Amide II) demonstrated the existence of helical structure of collagen as reported by Riaz et al. [22] and Azis et al. [23]. FTIR analysis was carried out to identify the possible biomolecule responsibility for capping and as efficient stabilizer of the metal nanoparticles synthesis by neem leaves extracts [24]. Figure 1 a shows functional groups surrounding AgNPs. The peak at 1668 cm^{-1} resembles the amide I. Meanwhile, the peak at 2140 cm^{-1} can be assigned to the alkyne group present in phytoconstituents of neem extracts.

Figure 2 shows the FTIR spectra of FsHA/FsCol/AgNPs and porous FsHA/FsCol/AgNPs composite beads with collagen respectively. FsCol samples showed two major peaks with a high intensity were identified at 1027 and 537 cm^{-1}. These corresponding to the phosphate group along with the minor peaks with low intensity which were observed at 1658 cm^{-1}, 1438 cm^{-1}, 1086 cm^{-1}, and 638 cm^{-1}. They referred to amide I (CO stretching), amide II (CH_2 bending) [25], Phosphate (PO_4^{-3}) and OH (hydroxyl group) groups, respectively [20,21].

The presence of FsCol in the matrix of FsHA beads can be proven by the appearance of weak peaks with a low intensity that was subordinate for amide I and amide II for AgNPs as mentioned in the FTIR spectrum of AgNPs (Figure 2) which was identified in the presence of functional group at 1640 cm^{-1}.

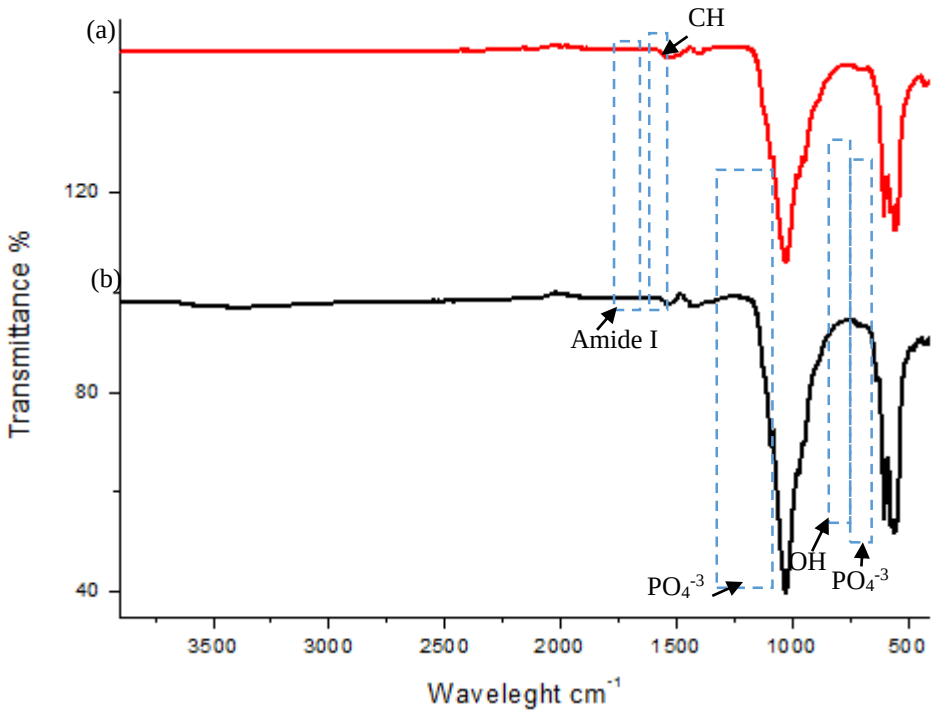

Figure 2. FTIR specturm of a) FsHA/FsCol/AgNPs and b) Porous FsHA/FsCol/AgNPs beads

SEM analysis of FsHA/FsCol/AgNPs beads. Figure 3(a) and (b) show the SEM morphology of FsHA/FsCol/AgNPs with and without starch. Porosity of composites treated with starch was observed in figure 1 (b) and supported by previous results. Infusion of pore composites with FsCol-AgNPs has been analysed as shown in Figure 3. These two samples were with FsCol/AgNPs. The porosity of FsHA beads have been identified in the SEM analysis, the samples with starch has been shown high porosity compared with the FsHA without starch. The present study has been aimd to enhance the porosity of the FsHA beads by add the starch and that target has been acheived.

A present of AgNPs particles were identified in the surface of beads with a spherical shape and a well distributed as shown in Figure 4. The diameter of silver nanoparticles was measured to be 18.22 nm to 35.68 nm. The results confirmed the ability of collagen chain together with silver nano particles to pass through the surface of porous bead during infiltration procedure.

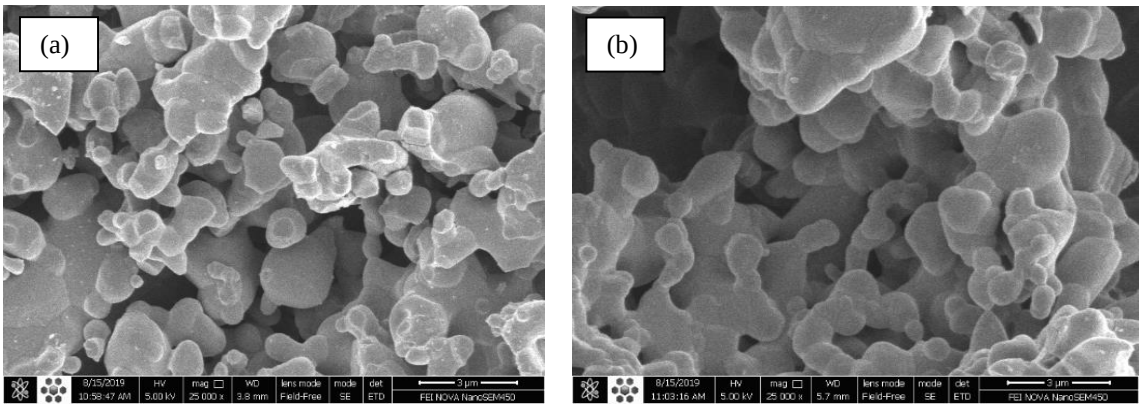

Figure 3. SEM Images of (a) FsHA/ FsCol/AgNPs and (b) Porous FsHA/ FsCol/AgNPs

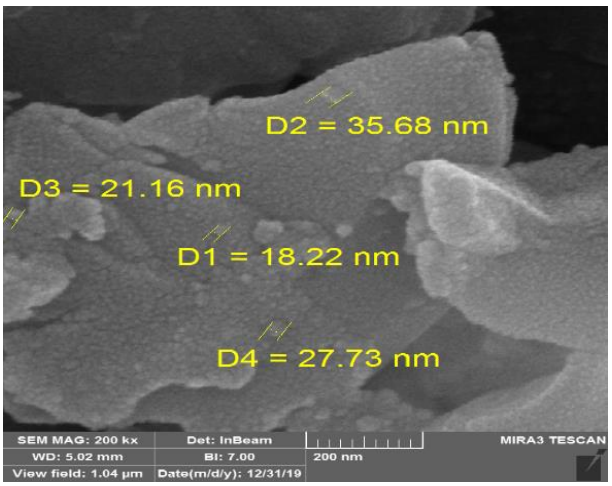

Figure 4. High magnification SEM of porous FsHA/FsCol/AgNPs

EDX of FsHA/FsCol/AgNPs beads. Figure 5 (a) and (b) show EDX spectra of FsHA/ FsCol/AgNPs and porous FsHA/ FsCol/AgNPs. The elements that were observed in the samples are calcium (Ca), phosphor (P), and oxygen (O), along with other elements that were present in a small percentage, such as magnesium (Mg), aluminium (Al), and silicon (Si). In the previous studies, they have reported the presence of these elements in the hydroxyapatite that was extracted from fish [26]. The percent of AgNPs was identified to be available inside the beads of fish hydroxyapatite with a spherical shape and a homogeneously distributed on the surface of sample. AgNPs had been approximately identified at 3 keV in the FsHA/ FsCol/AgNPs and Porous FsHA/ FsCol/AgNPs.

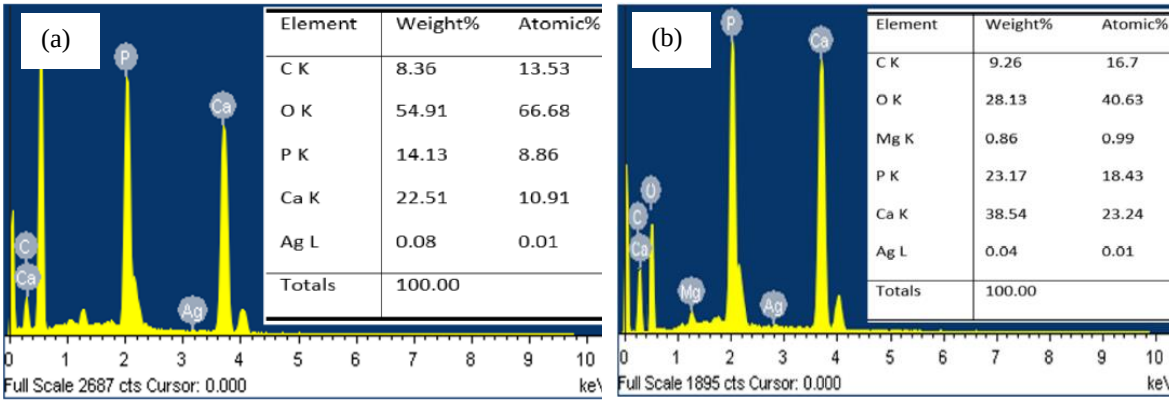

Figure 5. EDX Spectra a) FsHA/ FsCol/AgNPs and b) Porous FsHA/ FsCol/AgNPs

In a study by Morra et al. [27], their report of preparing HA/β-TCP/Col beads and characterising using XPS have shown the presence of calcium (Ca), phosphor (P), oxygen (O), carbon (C), and nitrogen (N). These elements were identified to be present with the HA and Col in the beads. In the present study, the same main elements have been identified to be present in the EDX results. Based on literature, no report on the preparation of HA/Col composite incorporating with silver nanoparticles using infiltration method have been published. The current study has shown the presence of AgNPs in the EDX analysis along with the presence of HA and collagen elements. This indicates that the aim of the present study to incorporate AgNPs particles together with collagen in HA beads to obtain HA/Col/AgNPs beads has been achieved.

XRD of FsHA/ FsCol/AgNPs beads. Figure 6 shows the XRD patterns that display several characteristic peaks of HA that are in perfect agreement with the previous studies [28]. The composite beads with AgNPs are shown in Figure 6 (a) and (b). The XRD analysis of these beads was carried out to identify the standard peaks of FsCol and AgNPs inside the FsHA bead matrix. The major peaks of FsHA beads were observed in the XRD pattern at 2θ value of 32.08°, 34.24°, 39.69°, and 47.18° [29]. For collagen, the peaks were observed at 25.39° and 12.32° [30]. The silver nanoparticles were identified to be present inside the matrix of beads. Two mean of peaks that belonged to the silver nanoparticles were observed at around 37.24° and 64.89° degrees (2θ) [31].

Diffraction peaks of FsCol were identified in the FsHA bead matrix at 20.24 [32] and 25.98 [33] degrees (2θ) and were referred to the FsCol. AgNPs were indicted available in the FsHA/FsCol/AgNPs and porous FsHA/FsCol/AgNPs beads. The narrow diffraction peaks were indicative of a crystalline material in these beads. 37.24 And 65.12 degrees (2θ) were identified for silver nanoparticles. In the present study, the new procedure was used to incorporate AgNPs and FsCol by making them penetrate the porosity of FsHA beads and distributing in the matrix of beads. According to the results and based on the explanation above, the objective of this study has been achieved.

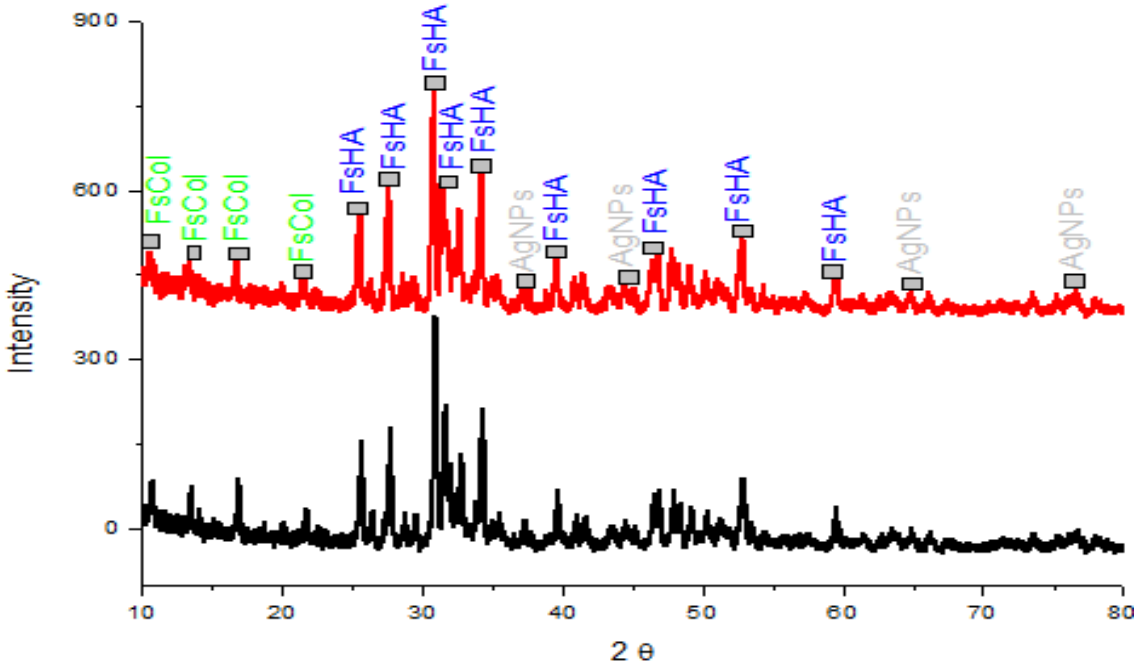

Figure 6. **XRD patterns of a) FsHA/FsCol/AgNPs and b) porous FsHA/ FsCol/AgNPs beads**

Conclusion

In the present study the FsHA/FsCol/AgNPs composites beads were prepared by infiltration of FsHA with FsCol-AgNPs solution. The results had revealed that by using XRD and FTIR analysis, the peaks of functional groups of FsCol and AgNPs were observed in the matrix of FsHA beads. FESEM had shown the morphology of beads with intact to the availability of silver nanoparticles on the surface of porous structure. The composites has been successfully prepared and characterized, the composites can be used in the bone filler applications.

Acknowledgements

This research was funded using FRGS Grant No. 2019-0147-103-02, Lab of Polymer, Department of Chemistry, Faculty of Science and Mathematics, UPSI, Perak, Malaysia.

Author Contributions

All authors contributed toward data analysis, drafting and critically reviewing the paper and agree to be account able for all aspects of the work.

Disclosure of Conflict to Interest

The authors have no disclosures to declare.

Compliance with Ethical Standards

The work is compliant with ethical standards.

References

[1] Borciani, G., Montalbano, G., Baldini, N., Cerqueni, G., Vitale-Brovarone, C., & Ciapetti, G. (2020). Co–culture systems of osteoblasts and osteoclasts: Simulating in vitro bone remodeling in regenerative approaches. *Acta biomaterialia*, 108 22-45

[2] Tal, R., Kisa, J., Abuwala, N., Kliman, H. J., Shaikh, S., Chen, A. Y., & Taylor, H. S. (2021). Bone marrow-derived progenitor cells contribute to remodeling of the postpartum uterus. *STEM CELLS*.

[3] Mudhafar, M., Zainol, I., Alsailawi, H. A., & Aiza Jaafar, C. N. (2021). Synthesis and characterization of fish scales of hydroxyapatite/collagen–silver nanoparticles composites for the applications of bone filler. *Journal of the Korean Ceramic Society*, 1-11.

[4] Weivoda, M. M., Chew, C. K., Monroe, D. G., Farr, J. N., Atkinson, E. J., Geske, J. R., & Khosla, S. (2020). Identification of osteoclast-osteoblast coupling factors in humans reveals links between bone and energy metabolism. *Nature communications*, 11(1) 1-13.

[5] Sobanko, J. F., Portilla, N., Etzkorn, J., Shin, T., & Miller, C. J. (2018). Repair of a Hemiforehead Defect With Exposed Bone. *Dermatologic Surgery*, 44(12) 1587-1590.

[6] Zhou, H., Lawrence, J. G., & Bhaduri, S. B. (2012). Fabrication aspects of PLA-CaP/PLGA-CaP composites for orthopedic applications: a review. *Acta biomaterialia*, 8(6) 1999-2016.

[7] Martins, A. M., Alves, C. M., Kasper, F. K., Mikos, A. G., & Reis, R. L. (2010). Responsive and in situ-forming chitosan scaffolds for bone tissue engineering applications: an overview of the last decade. *Journal of Materials Chemistry*,20(9) 1638-1645.

[8] Yelten-Yilmaz, A., & Yilmaz, S. (2018). Wet chemical precipitation synthesis of hydroxyapatite (HA) powders. *Ceramics International*, 44(8) 9703-9710.

[9] Granito, R. N., Renno, A. C. M., Yamamura, H., de Almeida, M. C., Ruiz, P. L. M., & Ribeiro, D. A. (2018). Hydroxyapatite from fish for bone tissue engineering: A promising approach. *International journal of molecular and cellular medicine*, 7(2) 80.

[10] Mondal, S., Mondal, B., Dey, A., & Mukhopadhyay, S. S. (2012). Studies on processing and characterization of hydroxyapatite biomaterials from different bio wastes. *J. Miner. Mater. Charact. Eng*, 11(1) 55-67.

[11] Dutta, S. R., Passi, D., Singh, P., & Bhuibhar, A. (2015). Ceramic and non-ceramic hydroxyapatite as a bone graft material: a brief review. *Irish Journal of Medical Science (1971-)*, 184(1) 101-106.

[12] Lin, F., Wang, X., Wang, Y., Yang, Y., & Li, Y. (2017). Preparation and biocompatibility of electrospinning PDLLA/β-TCP/collagen for peripheral nerve regeneration. *RSC advances*, *7*(66) 41593-41602.

[13] Xu, M., McCanna, D. J., & Sivak, J. G. (2015). Use of the viability reagent PrestoBlue in comparison with alamarBlue and MTT to assess the viability of human corneal epithelial cells. *Journal of pharmacological and toxicological methods*, 71 1-7.

[14] Villa, M. M., Wang, L., Rowe, D. W., & Wei, M. (2014). Effects of cell-attachment and extracellular matrix on bone formation in vivo in collagen-hydroxyapatite scaffolds. *PloS one*, 9(10) e109568.

[15] Rafat, M., Xeroudaki, M., Koulikovska, M., Sherrell, P., Groth, F., Fagerholm, P., & Lagali, N. (2016). Composite core-and-skirt collagen hydrogels with differential degradation for corneal therapeutic applications. *Biomaterials*, 83 142-155.

[16] Suchý, T., Bartoš, M., Sedláček, R., Šupová, M., Žaloudková, M., Martynková, G. S., & Foltán, R. (2021). Various Simulated Body Fluids Lead to Significant Differences in Collagen Tissue Engineering Scaffolds. *Materials*, 14(16) 4388.

[17] Sari, N. K., Indrani, D. J., Johan, C., & Corputty, J. E. M. (2017, August). Evaluation of chitosan-hydroxyapatite-collagen composite strength as scaffold material by immersion in simulated body fluid. In *Journal of Physics: Conference Series*, 884(1) 012116.

[18] Zhou, C., Ye, X., Fan, Y., Ma, L., Tan, Y., Qing, F., & Zhang, X. (2014). Biomimetic fabrication of a three-level hierarchical calcium phosphate/collagen/hydroxyapatite scaffold for bone tissue engineering. *Biofabrication*, 6(3) 035013.

[19] Lu, Z., Liu, S., Le, Y., Qin, Z., He, M., Xu, F., & Zheng, L. (2019). An injectable collagen-genipin-carbon dot hydrogel combined with photodynamic therapy to enhance chondrogenesis. *Biomaterials*, 218 119190.

[20] Muhammad, N., Gao, Y., Iqbal, F., Ahmad, P., Ge, R., Nishan, U., & Ullah, Z. (2016). Extraction of biocompatible hydroxyapatite from fish scales using novel approach of ionic liquid pretreatment. *Separation and Purification Technology*, 161 129-135.

[21] Ye, H., Liu, X. Y., & Hong, H. (2009). Characterization of sintered titanium/hydroxyapatite biocomposite using FTIR spectroscopy. *Journal of Materials Science: Materials in Medicine*, 20(4) 843-850.

[22] Riaz, T., Zeeshan, R., Zarif, F., Ilyas, K., Muhammad, N., Safi, S. Z., & Rehman, I. U. (2018). FTIR analysis of natural and synthetic collagen. *Applied Spectroscopy Reviews*, 53(9) 703-746.

[23] Aziz, J., Ahmad, M. F., Rahman, M. T., Yahya, N. A., Czernuszka, J., & Radzi, Z. (2018). AFM analysis of collagen fibrils in expanded scalp tissue after anisotropic tissue expansion. *International journal of biological macromolecules*, 107 1030-1038.

[24] Devaraj, P., Kumari, P., Aarti, C., & Renganathan, A. (2013). Synthesis and characterization of silver nanoparticles using cannonball leaves and their cytotoxic activity against MCF-7 cell line. *Journal of nanotechnology*, 2013.

[25] Pati, F., Adhikari, B., & Dhara, S. (2010). Isolation and characterization of fish scale collagen of higher thermal stability. *Bioresource technology*, 101(10) 3737-3742.

[26] Abifarin, J. K., Obada, D. O., Dauda, E. T., & Dodoo-Arhin, D. (2019). Experimental data on the characterization of hydroxyapatite synthesized from biowastes. *Data in brief*, 26 104485.

[27] Morra, M., Giavaresi, G., Sartori, M., Ferrari, A., Parrilli, A., Bollati, D., & Fini, M. (2015). Surface chemistry and effects on bone regeneration of a novel biomimetic synthetic bone filler. *Journal of Materials Science: Materials in Medicine*, 26(4) 159.

[28] Sena, L. A., Caraballo, M. M., Rossi, A. M., & Soares, G. A. (2009). Synthesis and characterization of biocomposites with different hydroxyapatite–collagen ratios. *Journal of Materials Science: Materials in Medicine*, 20(12) 2395.

[29] Alparslan, Y., Baygar, T., & Baygar, T. (2017). Extraction, characterization and antimicrobial activity of hydroxyapatite from seabass and seabream scale. *Food and Health*, 3(3) 90-96.

[30] Chinh, N. T., Manh, V. Q., Trung, V. Q., Lam, T. D., Huynh, M. D., Tung, N. Q., & Hoang, T. (2019). Characterization of collagen derived from tropical freshwater carp fish scale wastes and its amino acid sequence. *Natural Product Communications*, 14(7) 1934578X19866288.

[31] Saxena, A., Tripathi, R. M., Zafar, F., & Singh, P. (2012). Green synthesis of silver nanoparticles using aqueous solution of Ficus benghalensis leaf extract and characterization of their antibacterial activity. *Materials letters,* 67*(*1) 91-94.

[32] Liao, W., Guanghua, X., Li, Y., Shen, X. R., & Li, C. (2018). Comparison of characteristics and fibril-forming ability of skin collagen from barramundi (Lates calcarifer) and tilapia (Oreochromis niloticus). *International journal of biological macromolecules*, 107 549-559.

[33] Yoshida, S., Sudo, T., Niimi, M., Tao, L., Sun, B., Kambayashi, J., & Matsuoka, H. (2008). Inhibition of collagen-induced platelet aggregation by anopheline antiplatelet protein, a saliva protein from a malaria vector mosquito. *Blood, The Journal of the American Society of Hematology*, 111(4) 2007-2014.